ChemComm

Accepted Manuscript

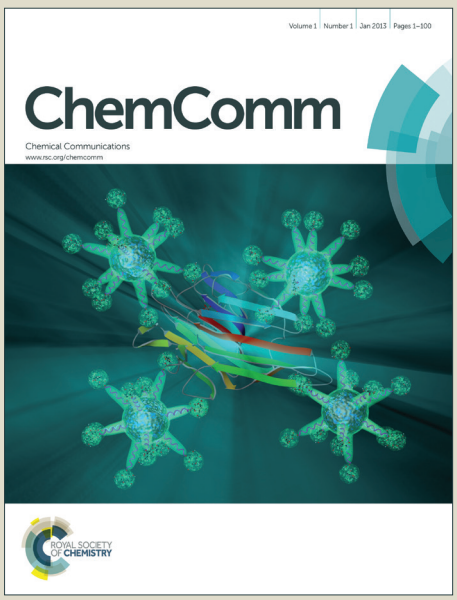

ROYAL SOCIETY OF CHEMISTRY

www.rsc.org/chemcomm

Chemical Communications

RSCPublishing

FEATURE ARTICLE

From Stereodynamics to High-Throughput Screening of Catalysed Reactions

Cite this: DOI: 10.1039/x0xx00000x

Skrollan Stockinger,[a] Julia Gmeiner,[a] Kerstin Zawatzky,[a] Johannes Troendlin[a] and Oliver Trapp[a*]

Received 00th January 2012,
Accepted 00th January 2012

DOI: 10.1039/x0xx00000x

www.rsc.org/

Characterising chemical reactions by kinetic analysis is of fundamental importance to experimentally obtain insights into reaction mechanisms. Based on such investigations reactions can be optimized and improved catalysts designed. Enhanced reaction conditions may drastically increase the performance of the reaction in terms of yield and (enantio-) selectivity. Understanding reaction kinetics in more complex systems involving adaptive chemical and dynamic systems on a molecular level as shown here is even more challenging. Here we review recent developments in monitoring reactions including the dynamic interconversion of stereoisomers by integrating (catalysed) reactions and chemical analysis in on-column reaction chromatographic devices. These recent developments allow rapid screening of reactions in great detail and are a central tool in determining reaction pathways and to understand how to control the stereodynamics of chiral molecules.

Introduction

Profound knowledge of the mechanism of a (catalytic) reaction is of great importance. It constitutes the basis for expanding and optimising the spectrum of synthetic applications as well as developing sustainable chemical processes in industrial applications. A key step for this approach is to obtain detailed information about the transition states of reactions and to find ways of controlling them. This allows an optimised design of new catalysts as well as a general advancement of the desired synthesis. Because such investigations can be a very tedious and time-consuming task, it is desirable to find new and improved techniques for the comprehensive experimental study of reactions and the (stereo-)dynamics of molecules,[1] and especially the individual pathways of stereoselective transformations.

The general procedure commonly used today to obtain reaction kinetics is employing batch reactors (e.g. flasks). This one-reaction-per-run approach usually requires large quantities (mg to g amounts) of pure substrates, catalysts and sometimes product(s) to verify the desired conversion. Reaction, separation, quantification as well as kinetic analysis are in most cases performed consecutively. Systematic investigations of multiple reaction conditions or an array of substrates is accordingly rather time and labour intensive.

Combining reaction and analysis in one single, miniaturized step would therefore be a great relief for all types of kinetic and mechanistic investigations.[2] Already in use are microfluidic devices such as flow-through micro reactors.[3-7] These types of devices are increasingly used in synthetic organic chemistry,[8-14] as well as in micro total analysis systems (μTAS) such as lab-on-a-chip.[15-20] They are not only used for automatically performed computer-controlled analytical operations but also for the high-throughput screening of reactions to determine conversions and catalytic activities.[21-23] Such miniaturized microfluidic devices not only offer the advantage of large surface-to-volume ratios, but also allow a precise control of the temperature, which is the key requirement for obtaining reliable kinetic data. Quartz chips and fused silica capillaries have the greatest potential for these applications because of their high thermal conductivity. Thus even highly exergonic reactions can be analysed with superior precision. Using such devices even multiphase catalytic systems, which are of great interest for industrial processes, are accessible.[24] Typically in multiphase systems the interaction of the reactant with the catalyst is controlled by mass transfer between the different phases resulting in a reaction rate which is composed of the inherent reaction rate and the diffusion rate. Increasing the interfacial area in such systems reduces the contribution of the diffusion rate to the overall rate constant. For circular reaction channels the interfacial area per volume α_{inter} only depends on the radius (r)

$$\alpha_{inter} = 2/r \quad (1)$$

For instance, the specific interfacial area per volume of capillaries with an inner diameter between 100 and 250 μm ranges from 16.000 to 40.000 m^2/m^3.[24]

Despite the enormous progress that was made in recent years, there are still many experimental challenges such as the efficient control of mixing, interfacing with analytical instruments[25] or uniform modification of reaction channels with immobilized catalysts. This is especially true for the square or rectangular shaped reaction channels commonly used in microfluidic devises. These are often closed by a cover glass glued on top of the chip, and are difficult to coat in a uniform manner because of the shape and the different materials (glue and glass/ silica/ polymer) used. Yet, even small deviations in the thickness lead to non-linear behaviour. For micro capillaries this problem was solved by Grob *et al.*,[26] who established a robust coating procedure that allows creating polymeric films with defined thickness.

Micro capillaries are routinely applied in gas chromatography (GC), open-tubular liquid chromatography (OTLC) and capillary electrophoresis (CE). Capillary based analytical devices allow performing reactions and analysis in the same or consecutive columns. Combining catalytic activity and separation selectivity in a single or consecutive micro reactor column offers many advantages, such as the possibility to investigate degenerated interconversion processes such as the interconversion of stereoisomers by dynamic chromatography[27-31] or reactions in a high-throughput fashion under exactly the same reaction conditions.[32] Such measurements are of interest in many fields, ranging from lead structure optimization of catalysts to the measurement of the stereointegrity of drugs.[33-38] Furthermore by combining reaction and separation there is the opportunity to shift equilibria of reactions to the side of the reaction products, resulting in an improved conversion compared to reactions conventionally performed in a flask. Besides the reaction kinetics, micro capillary based reaction chromatography also yields information about chromatographic adsorption and diffusion parameters.[39]

In on-column reaction chromatography every theoretical plate of the separation column can be considered as a chemical micro reactor according to the theoretical plate model of chromatography. In this model a column consists of N theoretical plates (cf. Fig. 1). The interaction in the stationary phase consists of the contributions of physisorption (distribution between the gas and the stationary phase) and chemisorption (distribution of the reactants and products between the dissolved state and the reactant-product-complex state within the stationary liquid phase).

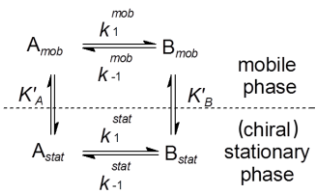

Fig. 1 Equilibrium in a single chromatographic theoretical plate.

Tamaru *et al.* published the first example of an integrated on-column setup combining catalysis and chromatographic separation. In their experiment palladium deposed Celite 545 was packed in a GC column to study the decomposition of formic acid.[40] In the following years Bassett and Habgood[41] analysed the isomerization of cyclopropane to propylene as first-order reaction and Gil-Av and Herzberg-Minzly[42] investigated Diels-Alder reactions as example for a second-order reaction. These authors impregnated the stationary phase of a GC column with the dienophile and injected various dienes, resulting in non-volatile Diels-Alder adducts, remaining on the separation column. The retro Diels-Alder reaction of *endo*-dicyclopentadiene was investigated by Langer *et al.*,[43] leading to an extension of the concept of chromatographic reactors, and by Marriott *et al.*,[44] who compared packed and capillary columns. The latter group also found that packed columns with larger diameters were more efficient than coated capillaries. However, the specific interfacial area per volume is dramatically higher for coated capillary columns than those of packed columns. As catalysed reactions as well as separations are governed by high surface areas, it can be concluded that coated capillaries should be favoured. A number of decomposition experiments were investigated by Matsen *et al.*,[45] who used Pt on alumina support as catalyst, and Skrdla who performed thermally initiated reactions.[46] Both groups found, that in on-column reaction chromatographic systems the conversion is increased as compared to equilibrium conditions. They also concluded that this new approach, utilizing peak area measurements is faster, more robust and accurate than conventional chromatographic measurements.

In the following more recent developments of stereodynamic analysis as well as combinations of catalytic transformation and separation in a single chromatographic capillary micro reactor are presented.

Determination of Kinetic Data

Data Evaluation Models

For the kinetic evaluation of on-column reaction chromatographic (ocRC) experiments different theoretical models can be applied. The classical method is the determination of the conversion from the integrated peak areas of the chromatogram, corrected by the response factors of each compound, which are determined by calibration measurements. For first-order reactions the following equation 2 can be used to determine the reaction rate constant:

$$[E] = ([P] + [E])e^{-k\Delta t} \qquad (2)$$

For a first-order reaction the reactant E is converted into the product P within the reaction time t, which equals the contact time Δt determined by comparable measurements with and without catalytically active capillary. Equation 2 can be expanded to any other reaction rate law.

Another approach is described by the theoretical plate model. This model was originally developed to describe a separation process based on partitioning. Thus, the separation in a column

is described as a discontinuous process whereas all steps are repeated in separate uniform sections of a multi-compartmentalized column consisting of N theoretical plates.[47-49] For an on-column reaction every theoretical plate is considered as a distinct chemical reactor (cf. Fig. 1).[50-53] In case of irreversible reactions the reaction scheme can be simplified by negating k_{-1}^{mob} and k_{-1}^{stat} and for catalysed reactions the contribution of the reaction in the mobile phase can also be neglected (k_1^{mob} and k_{-1}^{mob}). In this model the reactant species are distributed between the mobile and the stationary phase, where they undergo (inter-) conversion. The content of the mobile phase is shifted to the subsequent theoretical plate, whereas the stationary phase is retained. While the given amount of enantiomers is initially introduced in the system on the first theoretical plate, the content of the mobile phase of the last theoretical plate is finally recorded as a chromatogram featuring a(n) (inter-) conversion profile over the time t.

Based on Gaussian distribution functions of the non-interconverted stereoisomers $\Phi(t)$ and with a time dependent probability density function $\Psi(t)$ to describe the conversion profile, a stochastic model of the theoretical plate model could be introduced.[54] On basis of the unified equation of chromatography (Eq. 3a and 3b) it is possible to determine reaction rate constants of any first-order reaction directly from chromatographic elution profiles without the need of a tedious reaction progress analysis.[55,56] Therefore equation 3a has to be applied if the first eluted peak (A) is higher than the second eluted peak (B) and equation 3b for an opposite elution profile (B>A).

$$k_1^{ue} = -\frac{1}{t_R^A}\left(\ln\left(B_0 e^{-\frac{A_\infty}{B_\infty}k_1^{ue} t_R^i}\left(\frac{100e^{-\frac{(t_R^B-t_R^A)^2}{8\sigma_B^2}} - h_p e^{-\frac{(t_R^B-t_R^A)^2}{2\sigma_B^2}}}{\sigma_B\sqrt{2\pi}} - \frac{100}{t_R^B-t_R^A}\right) + \frac{100B_0 + A_0\left(100 - h_p\left(1+\sqrt{\frac{2}{\pi N}}\right)\right)}{t_R^B - t_R^A}\right) - \ln\left(A_0\left(\frac{h_p - 100e^{-\frac{(t_R^A-t_R^B)^2}{8\sigma_A^2}}}{\sigma_A\sqrt{2\pi}} + \frac{100 - h_p\left(1+\sqrt{\frac{2}{\pi N}}\right)}{t_R^B - t_R^A}\right)\right)\right) \quad (3a)$$

$$k_1^{ue} = -\frac{1}{t_R^A}\left(\ln\left(B_0 e^{-\frac{A_\infty}{B_\infty}k_1^{ue} t_R^i}\left(\frac{100e^{-\frac{(t_R^A-t_R^B)^2}{8\sigma_B^2}} - h_p + \frac{h_p\left(1-\sqrt{\frac{2}{\pi N}}\right)-100}{t_R^B-t_R^A}}{\sigma_B\sqrt{2\pi}}\right) + \frac{100A_0 + B_0\left(100 - h_p\left(1-\sqrt{\frac{2}{\pi N}}\right)\right)}{t_R^B - t_R^A}\right) - \ln\left(A_0\left(\frac{h_p e^{-\frac{(t_R^B-t_R^A)^2}{2\sigma_A^2}} - 100e^{-\frac{(t_R^B-t_R^A)^2}{8\sigma_A^2}}}{\sigma_A\sqrt{2\pi}} + \frac{100}{t_R^B - t_R^A}\right)\right)\right) \quad (3b)$$

with

$$\sigma_i = \frac{w_i}{\sqrt{8\ln 2}} \quad ; i = A \text{ or } B$$

k = reaction rate constant
h_p = plateau height at the mean retention time
A_0/B_0 = concentration of A or B
t_R = retention time
N = theoretical plate number
w = peak width

The unified equation of chromatography (Eq. 3a and 3b) allows the direct calculation of reaction rate constants k_1 and k_{-1} and Gibbs activation energies $\Delta G^{\ddagger}$ for all types of first-order reactions taking place in chromatographic or electrophoretic systems, regardless of the initial concentrations of the reactants A and B and the equilibrium constant $K_{A/B}$. The Gibbs free activation energy $\Delta G^{\ddagger}(T)$ can be calculated according to the Eyring equation (Eq. 4, with the Boltzmann constant (k_B = 1.380662x10^{-23} J·K^{-1}), T as the reaction temperature [K], the Planck's constant (h = 6.62617·10^{-34} J·s) and the gas constant (R = 8.31441 J·K^{-1}·mol^{-1})). The statistical factor κ is normally unknown and set to 1.0.

$$\Delta G^{\ddagger}(T) = -RT\ln\left(\frac{k_1 h}{\kappa k_B T}\right) \quad (4)$$

The activation enthalpy $\Delta H^{\ddagger}$ is then obtained from the slope and the activation entropy $\Delta S^{\ddagger}$ from the intercept of the Eyring plot ($\ln(k_1/T)$ as a function of T^{-1}).

Stereodynamics of Disubstituted BIPHEPs

The activation parameters ($\Delta G^{\ddagger}$, $\Delta H^{\ddagger}$ and $\Delta S^{\ddagger}$) are important values for an improved comparison of derivatives for instance of different substituted ligands for asymmetric catalysis. An in depth understanding of all influencing factors which affect the stereodynamics of ligands and thereby the catalysis is a requirement for good catalyst design as well as for a better understanding of the reaction and interaction mechanism.

An example of how such investigations can support synthesis by improving the catalyst through an optimized ligand system and substitution pattern is given by Trapp et al.[57-59] In their study the activation parameters allowed a comparison of the stereodynamics of 3,3'-, 5,5'- and 6,6'-disubstitued BIPHEP (2,2'-bis(diphenylphosphino)-biphenyls) ligands, based on their rotational barriers measured by enantioselective dynamic high-performance liquid chromatography (DHPLC). The unsubstituted BIPHEP showed the lowest rotation barrier with a Gibbs activation energy $\Delta G^{\ddagger}$ of 86.8 kJ·mol^{-1} (Fig. 2). To investigate the influence of the ligand-substitution pattern several dimethoxy-substituted BIPHEPs were investigated. The rotational barrier of the 6,6'-disubstited ligand was found to be significantly higher than that of the 3,3'- or 5,5'-disubstited analogue (cf. Fig. 2). This atropisomeric behaviour was attributed to steric hindrance and even present at elevated temperatures. The rotational barrier of the 3,3'-disubstituted BIPHEP was found to be slightly higher than that of the 5,5'-disubstituted ligand possibly due to a buttressing effect that increases the steric hindrance along the σ bond.[60] Next, the

influence of different substituents within the same substitution scheme was also compared. Interestingly, the activation barriers were in a narrow range between 87.8 and 93 kJ·mol^{-1}, which was explained by enthalpy and entropy compensations.[61] All the BIPHEPS investigated (except the 6,6'-disubstituted) retained their tropos properties at room temperature.

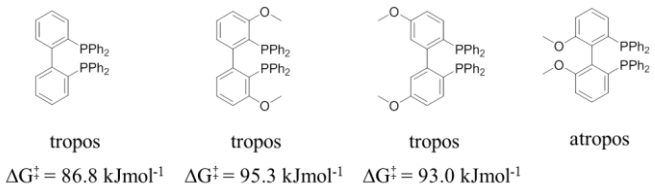

Fig. 2 Comparison of the Gibbs free activation energy determined based on the rotation barrier of BIPHEP ligands with different substitution pattern.[57]

Stereodynamics of Small 1,2-Dialkyldiaziridines

Another example where kinetic data can help to explain experimental findings is shown in the field of stereogenic nitrogen. There, especially the interconversion barrier of 1,2-dialkyldiaziridines is of interest.[62-65] 1,2-Dialkyldiaziridines exhibit a high stereointegrity, because the lone electron pairs of the nitrogen atoms retain the structures in trans configuration, avoiding repulsive electron and steric interaction. Yet, due to the limited stereointegrity of the chirotopic nitrogen atom the two stereoisomers (enantiomers) are interconverting. A detailed investigation of the stereodynamics showed that among these 1,2-dialkyldiaziridines derivatives the ones equipped with small substituents exhibit rather high interconversion barriers despite the absence of sterically demanding substituents. This could be explained by the destabilization of the transition state of interconversion. The activation parameters for small 1,2-dialkyldiaziridines bearing ethyl-, *iso*propyl- and *tert*butyl-substituents were determined using enantioselective dynamic gas chromatography (DGC) (Fig. 3).[66] The ethyl substituted diaziridine showed the lowest rotational barrier whereas both sterically demanding groups (*iso*propyl- and *tert*butyl-) provided very similar values. Consequently, the steric differences between the *iso*propyl- and the *tert*butyl-substituent are too small to cause a significant effect on the Gibbs activation energy $\Delta G^{\ddagger}$.

R = Et	-	$\Delta G^{\ddagger}$ = 124.4 kJmol^{-1}
R = *i*Pr	$\Delta G^{\ddagger}$ = 125.9kJmol^{-1}	$\Delta G^{\ddagger}$ = 129.0kJmol^{-1}
R = *t*Bu	$\Delta G^{\ddagger}$ = 127.2kJmol^{-1}	$\Delta G^{\ddagger}$ = 129.1kJmol^{-1}

Fig. 3 Comparison of the Gibbs free activation energy of different substituted 1,2-dialkyldiaziridines.[66]

On-column Reaction Chromatography

On-column reaction chromatography for kinetic investigations is generally performed in three steps (i) pre-separation (ii) reaction (iii) analysis. If the catalytically active reaction capillary acts as separation capillary at the same time the setup is simplified (Figs. 4a and 4b). In all other cases these steps take place in up to three columns (i) a catalytically active reactor capillary (catalytic column), (ii) a (post-) separation capillary and (iii) optionally a pre-separation capillary (Fig. 4c). The pre-separation column is used for thermal equilibration of the reactants (i.e. in GC: after injection into a hot injector), for separating reactant libraries, so that no competing intermolecular reactions occur as well as for removing impurities in the reactants in order to preserve the catalytic activity. The (post-) separation capillary is coated with a suitable (chiral) stationary phase for qualitative and quantitative analysis.

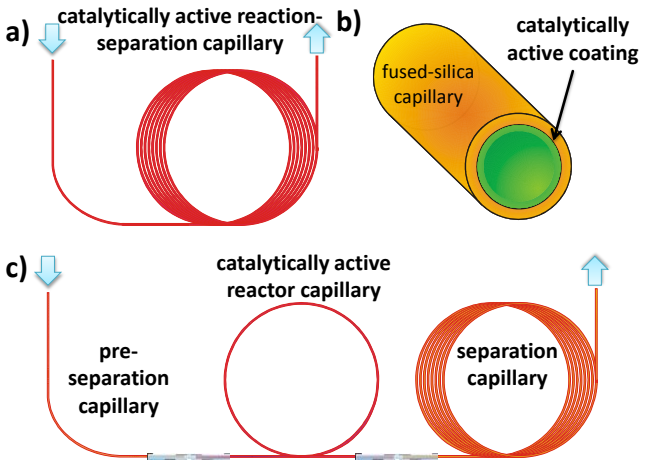

Fig. 4 On-column reaction chromatographic setup with a) integrated catalytic activity and separation selectivity in a single capillary, b) schematic cross-section of a fused silica capillary with a homogeneous wall coating of a catalyst dissolved in a polymeric liquid stationary phase, and c) consecutive performed catalytic transformation and separation.

For the preparation of capillary micro reactors as catalytically active columns or separation columns the static coating procedure, investigated by Grob can be used.[26] Therefore the suitable polymer with or without catalyst is dissolved in a volatile solvent, filled in the capillary and the solvent is slowly removed. The film thickness of the polymer can be regulated by varying the concentration of polymer and catalyst as well as by changing the inner diameter of the capillary (Fig. 4b). There are two common strategies to obtain a catalyst-containing polymer. One is to dissolve the catalyst in the polymer; the other is to covalently attach the catalyst to the polymeric network. For the covalent immobilization the catalyst is attached via a flexible linker to the polymer, e.g. polysiloxane (cf. Fig. 8). A major benefit of a covalently immobilized catalyst is the enhanced thermal stability and thus a decreased column bleed.

Alternatively the catalyst can be dissolved in the polymer, thus no coating-oriented syntheses has to be performed, resulting in a faster access to the catalytically active column and a direct comparison with the off-line measurements of this particular catalyst by conventional synthesis.[69] For all applications the choice of the stationary phase and the coating method has to be made carefully with regard to the specific reaction and the catalyst. In on-column reaction chromatography all reactions take place in the liquid stationary phase, thus all calculated reaction rate constants are absolutely comparable to their analogues, determined by reaction progress analysis,[67] where samples are periodically taken from a flask or conventional reactor.

High-Throughput Measurements

Classical on-column reaction chromatography combines reaction and analysis in a single step resulting in a significantly accelerated process compared to conventional reaction monitoring, which is usually performed by decoupled synthesis and analysis. In combination with a high-throughput approach the setup can be enhanced even further. In such a setup a library of reactants is simultaneously injected onto an on-column reaction chromatographic system. The detectable data can be analysed like single measurements if a sufficient characterization and separation is available. Using this approach kinetic analysis of multiple reactions can be realized under the exact same reaction conditions in virtually the same time frame of a single measurement of one reactant (Fig. 5). An essential requirement for this setup is a pre-separation column which separates the reactants before the catalytic reaction in order to prevent intermolecular side-reactions and support the separation selectivity of the resulting reactants and product mixture. The practical applicability of this approach was demonstrated for hydrogenations over highly active Pd nanoparticles[68] and the ring closing metathesis using Grubbs 2nd generation catalyst[69] achieving an extraordinary high throughput of up to 5880 reactions in only 40 hours!

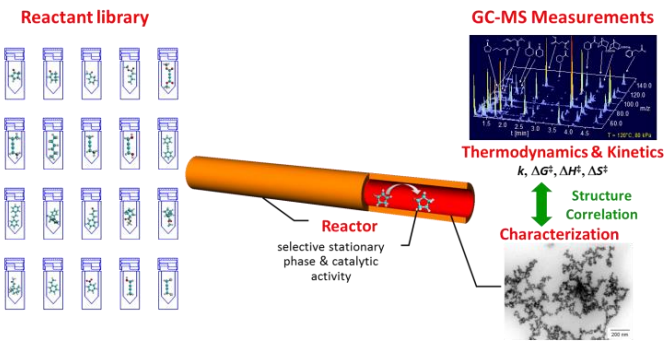

Fig. 5 Schematic overview of an on-column reaction chromatographic system containing a reactant library injected onto a catalytically active capillary followed by determination of the reaction kinetics on the basis of the unified equation for chromatographic systems.

Plenio *et al.* realised high-throughput kinetic studies to investigate the Sonogashira CC-coupling by simultaneous conversion of up to 25 different substrates in a single reaction vessel.[70] Thereby they could analyse almost 500 coupling reactions by comparing different sets of multi-substrate experiments whereas one property was permutated in every multi-substrate set (e.g. the substituent on a specified position, the whole substitution pattern or the ligand) to determine activation enthalpies and entropies as well as Hammett constants. Comparison of the results obtained by these multi-substrate experiments with conventional single-substrate experiments they could demonstrate that competitive effects were negligible. By one-pot multi-substrate experiments they elegantly solved the problem to keep the allocation of the analyser time constant for all compounds, which normally leads to intrinsic deviations in reaction time and consequently the conversion in conventional single-substrate experiments or parallel reactors.[71] Nevertheless these applications are still based on a separation of reaction products which requires a well-designed sample preparation as well as sampling strategy. Rothenberg *et al.* published a self-audited system, which determines the optimal analyser time based on extracted concentration profiles, thus reduces the analysis to a minimum.[71] But even in combination with such a smart self-audited system the analysis is still a consecutive and additional step, which can influence the reaction composition by continuous sampling to perform kinetic measurements. In contrast to this in the here presented on-column reaction chromatographic setup reaction and separation are integrated and allow to perform synthesis and analysis in a single step.

First-order Reactions

First-order reaction rate laws can be assigned to intramolecular reactions like interconversions, rearrangements and degradation reactions. Pseudo first-order reactions can be easily realized by adding one of the reactants in excess to the mobile phase, e.g. using hydrogen as reactive carrier gas for hydrogenations in GC,[69] or an additive in HPLC or CE, e.g. hydrogen peroxide as oxidant.[72]

Gosteli-Claisen Rearrangement

The Gosteli-Claisen rearrangement of stereoisomeric 2-alkoxycarbonyl-substituted allyl vinyl ethers is an excellent example for the applicability of enantioselective ocRGC for the kinetic analysis of asymmetric reactions.[73] In this rearrangement allyl vinyl ether **1** (Fig. 6) was used as reactant in an on-column reaction gas chromatographic system (Fig. 7).

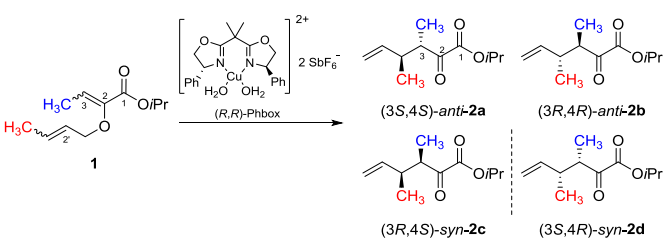

Fig. 6 Asymmetric Gosteli-Claisen rearrangement studied by on-column reaction gas chromatography (ocRGC; cf. Fig. 7).

What makes this reaction problematic to monitor is, that the allyl vinyl ether **1** undergoes an uncatalysed thermal Gosteli-Claisen rearrangement (Fig. 7b and c). These uncatalysed products **2a** and **2b**, formed by a thermally initiated rearrangement in the hot injector of the GC, can be used as internal standard to determine contact times between the reactants and the catalytically active capillary. The measurable time delay is caused by a spatially different formation of the thermally and catalytically formed δ,ε-unsaturated α-ketoesters on the column. As the product formed by the uncatalysed background reaction was separated from the residual allyl vinyl ether by the achiral pre-separation capillary both substrates eluted at different retention times onto the (*R*,*R*)-Phbox coated capillary where the stereoselective rearrangement took place. Consequently racemic and catalytic product were detected by the FID at different retention times making a direct differentiation of the thermally and catalysed formed product possible. Enantioselective GC using Chirasil-β-dex[74,75] as chiral stationary phase provided a good separation of the enantiomers formed by the uncatalysed and catalysed reactions, where the thermally formed species eluted first (cf. 7e and 7f). The catalyst (*R*,*R*)-Phbox (cf. Fig. 6) maintained its activity and selectivity within the investigated temperature range of 65 to 85°C. Within this range the activation parameters $\Delta H^{\ddagger}$ and $\Delta S^{\ddagger}$ as well as the Gibbs free activation energies $\Delta G^{\ddagger}(T)$ were determined with high precision. The best agreement in the calculation of reaction rate constants was achieved by applying a first-order reaction rate law for parallel reactions. For the rearrangement of **(*Z*,*E*)-1** to the major enantiomer **2b** the Gibbs free activation energy $\Delta G^{\ddagger}(T)$ at 80°C was determined to be 100.2±0.3 kJ·mol^{-1} and 104.2±0.3 kJ·mol^{-1} for the rearrangement to the minor enantiomer **2a**. Besides the advance of combined stereoselective catalysis and direct analysis of the reactants, this setup also allowed distinguishing directly between the stereoselectively catalysed reaction pathways and the non-stereoselective thermal ones. Due to the pre-separation of the competing reactants and the side reaction products both pathways could be simultaneously investigated and evaluated under exactly the same reaction conditions, leading to important kinetic information which can be used to optimize and tune reaction conditions and to improve mechanistic understanding. This setup is generally usable and thus transferable to a wide range of other on-column reaction chromatographic measurements.

Catalyst by the Meter

One advantage of permanently immobilized ligand systems is the possibility to form catalytically active capillaries by flushing the capillary with a suitable metal precursor solution. The highly versatile ligand class of *N*-heterocyclic carbenes (NHCs) constitutes such a catalytic ocRGC ligand system.[76] Using this system a broad range of reactions with superior properties in regard to stability and applicability in various reaction media and conditions can be investigated. There are different reaction pathways for the synthesis of the immobilized NHC ligands. An example of a suitable synthetic route is given by the synthesis of the permanently polymer bonded Grubbs 2nd generation catalyst (Fig. 8a). Generally a salt-free route is preferred for the synthesis of the immobilized ligand system; because decomposition of the ligand system, resulting from the use of a strong base to obtain the free carbene ligand, can be observed.[77] The immobilisable ligand can be synthesised using the common strategy of Blechert *et al.* (Fig. 8 i).[78] To

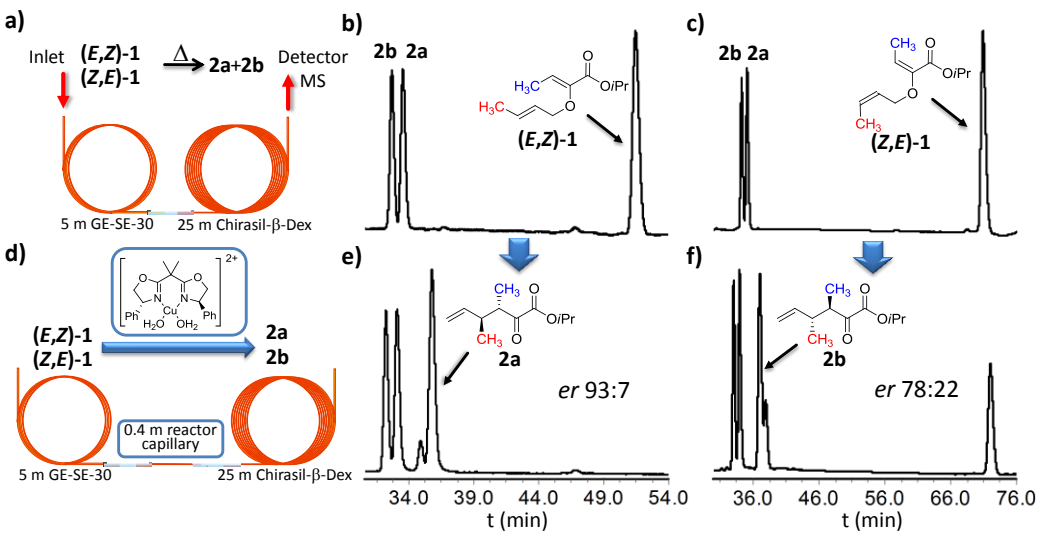

Fig. 7 Experimental setup of the stereoselective on-column gas chromatographic experiment to investigate the catalytic asymmetric Gosteli-Claisen rearrangement of (*E*,*Z*)- and (*Z*,*E*)-1 in absence (a) and presence (d) of the Lewis acid catalyst (*R*,*R*)-PhBox dissolved in an inert polysiloxane matrix (reactor capillary) to form the corresponding α-keto isopropyl esters 2a and 2b, respectively. Next to the respective setup representative chromatograms of the on-column experiment are shown (b, c: without reactor capillary; e, f: with reactor capillary; b, e: (*E*,*Z*)-1 as reactant; c, f: (*Z*,*E*)-1 as reactant). Adapted with permission from ref. [73], copyright 2011, American Chemical Society.

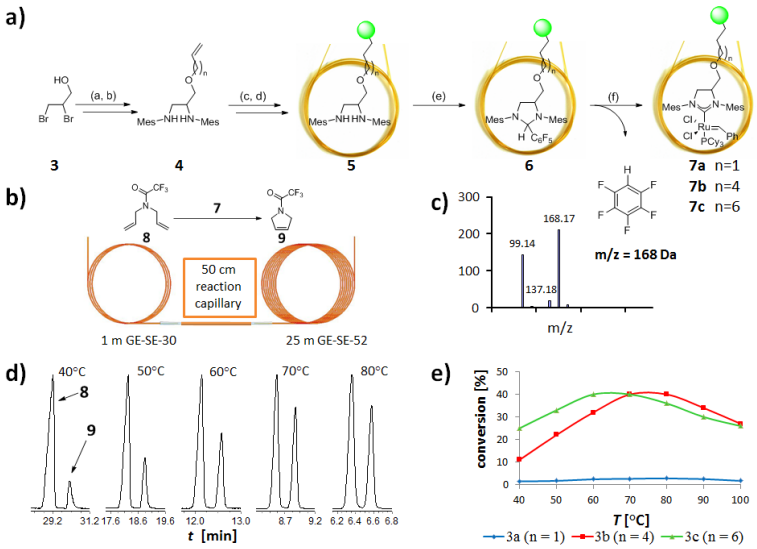

Fig. 8 a) Synthesis of the permanently immobilised diamine ligand **5** and conversion into the immobilised 1,3-dimesitylated imidiazolidine type carbene precursor **6**. (a) 2,4,6-Trimethylaniline, 120°C, 15 h. (b) NaH, ω-bromoalkene (n = 1, 4, 6), 78°C, 20 h. (c) Hydridomethyl-dimethylpolysiloxane (HMPS), Karstedt's catalyst, THF, sonication, 3 h (n = 1, 4, 6). (d) Fused silica capillary (i.d. 250 µm). (e) Pentafluorobenzaldehyde, AcOH, THF, rt, 20 h; (f) $(PCy_3)_2Cl_2RuCHPh$, n-pentane. b) Experimental setup: The reaction capillary is coupled between a pre-separation column (1m, GE-SE-30) and a separation column (25m, GE-SE-52). c) Mass spectrum of pentafluorobenzene released from **6** to monitor the formation of the free carbene by GC-MS. d) Elution profiles between 40°C and 80°C of the ocRGC ring closing metathesis experiment using *N*,*N*-diallyltrifluoroacetamide **8** as model substrate (first eluted peak) converted to *N*-trifluoroacetamide-3-pyrroline **9** (second eluted peak) using the catalyst column **7b** (n = 4). Helium was used as carrier gas (p = 80 kPa). e) Turnover of the on-column ring closing metathesis of *N*,*N*-diallyltrifluoroacetamide in dependence on the length n of the linker and the temperature T (p = 80 kPa Helium).

investigate the influence of the linker length in on-column reaction gas chromatography we introduced alkene chains with variable lengths. The coated diamine system was cyclised to achieve the carbene precursor **6** by taking advantage of solid phase chemistry. The *in-situ* formation of the carbene *via* thermal activation, and thus the ligand exchange reaction, can be controlled by GC/MS detection of the generated pentafluorobenzene. The immobilized version of the Grubbs 2nd generation catalyst was employed in the on-column ring closing metathesis of *N*,*N*-diallyltrifluoroactamide **8** to *N*-trifluoroacetamide-3-pyrroline **9** using the ocRGC setup depicted in Fig. 8 ii. We observed a strong dependence of the activity of the catalytic system on the spacer length. The maximum turnover of 40 % was monitored in combination with **7b** (at 80°C with n = 4) and **7c** (at 60°C with n = 6). In contrast to this the allyl linker system **7a** (n = 1) showed a turnover of only 4 % (Fig. 8e). The catalyst column gave stable measurements over a period of 24 hours using a wide temperature range (up to 150°C!).[76] Using the immobilised Grubbs 2nd generation catalyst with optimized spacer length (n = 4) we determined the activation parameters for the ring closing metathesis. The Gibbs activation energy $\Delta G^{\ddagger}$ (298 K) = 89.3 kJ·mol^{-1} is comparable with the activation parameters of the dissolved Grubbs 2nd generation catalyst, measured by on-column reaction chromatography in previous studies.[69] The experimentally determined data is also in accordance with experimental results of NMR experiments by Grubbs *et al.* which emphasises the applicability of this new approach.[79] Beside the analysed catalysts a great variety of NHC based complexes are conceivable and corroborate the flexibility and versatility of this ocRGC system. With these NHC pre-ligand modified fused-silica capillaries and potential suitable organometallic precursor complexes we are able to form promising catalytic systems. Another advantage of the preparation procedure of these catalytically active capillaries is that strategies can be applied well known from solid-phase chemistry, where high reagent concentrations can be applied to achieve high conversions in the synthesis of the ligands and the excess of reagents can be simply removed by flushing the capillaries with solvent. The possibility to produce several catalytically active capillaries at a time by simply increasing the length and cutting after modification inspired its description: catalyst by the meter.

Higher-order reactions

Unlike first-order reactions investigations of higher-order reactions require often a careful selection of the reaction parameters to be varied and in particular for on-column reaction chromatography. Common possibilities are sequenced injection of two reactants, where the second injected reactant moves faster and catch the first reactant inside the catalytically active

part, as well as a trapping of the reactants in a distinct part of the column arrangement. The time in which all reactants are combined is called contact time Δt. Matching injection times and contact times in presence of the catalyst is one of the challenges of the experiment-design of higher-order reactions. A possibility to overcome the mentioned challenges a cryogenic CO_2 cold trap may find its application in ocRGC.[80,81] Such a cryogenic cold trap is frequently used in GC applications to focus und concentrate samples, i.e. between columns in a multidimensional GC setup.[82,83]

As an example for a higher-order reaction the Diels-Alder reaction of benzenediazonium-2-carboxylate as benzene precursor with anthracene-9-derivatives toward triptycene-9-derivatives was investigated (Fig. 9).[80]

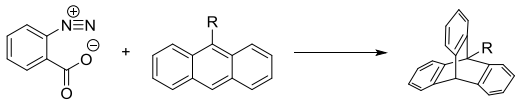

Fig. 9 Diels–Alder reaction of benzenediazonium-2-carboxylate with anthracene-9-derivatives giving triptycene-9-derivatives.

For this experiment a cooling trap was used to assist in focusing and mixing of the reactants in a defined area of the fused-silica capillary (Fig. 10a). The reactants were injected sequentially with different syringes to avoid undefined mixing in the injection port. The cryogenic cooling was kept at a constant temperature until 1 minute after the last injection (Fig. 10b). The cooling time as well as the injection order and intervals were optimized to achieve sufficient conversions at short reaction times. The transformation is thermally initiated, thus all columns are separation columns, a pre-column to thermally equilibrate the reactants after on-column cold injection and a following separation column whose first part is jacketed by the cryogenic CO_2 cooling trap. Considering the rather short reaction time this is a rather large amount, esp. in comparison to the 44 % yield of the off-line system which was formed after 3 hours at 80°C. In this experiment, the reaction time can be considered as the time between the end of the cryogenic cooling, after which the thawing of the reactants is initiated, and the chromatographic separation of the unreacted reactants and the product.

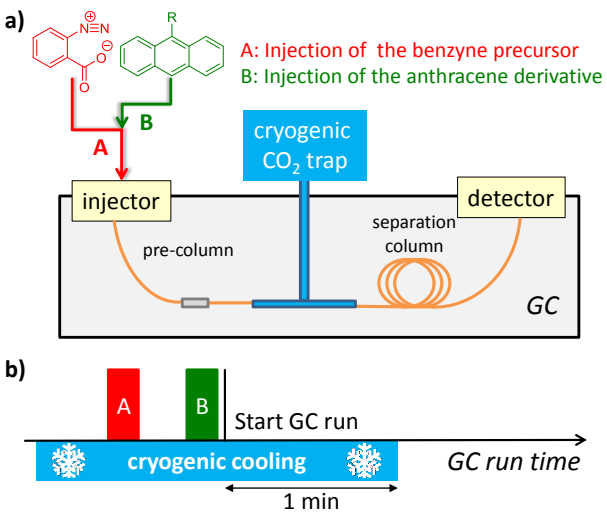

Fig. 10 a) The experimental setup of ocRGC to perform Diels-Alder reactions. b) Injection sequence protocol of the cryogenic ocRGC measurements. Reaction conditions: on-column cold injection, 60 °C for 5 min, then 6 °C/min to 180 °C, 120 kPa He; pre-column: fused silica, 10 cm, 250 nm film thickness, 250 µm i.d.; separation column: 10 m GE-SE30 (100% polydimethyl-siloxane), i.d. 250 µm, film thickness 500 nm.

The reaction rate constants were calculated based on the determined conversion and contact times Δt. Here the off-line reactions showed values between $8.4 \cdot 10^{-7}$ and $1.3 \cdot 10^{-5}$ s^{-1} whereas the ocRGC gave 1.4 to $6.2 \cdot 10^{-2}$ s^{-1}, an acceleration approximately 1000, three orders of magnitude. This drastic increase of the conversion rate clearly demonstrates the significance of the surface area on catalysed reactions. Despite the observed acceleration of the reaction, the reactivity is not affected by this reaction setup, both the off-line flask system and the ocRGC yielded the same reactivity order for substituted reactants. Consequently the presented ocRGC setup allows an accelerated investigation of higher-order reactions, avoiding the much slower off-line tests, yet yielding the same results. This setup is also applicable for other multi-order reactions provided the reactants and product are volatile to be measured by GC. It is also imaginable to use this setup to study individual reaction steps by cooling only locally at different positions of a catalytically active column.

A series of chemical transformations can be realised by coupling different catalytically active columns together. This has been demonstrated for ring-closing metathesis followed by the hydrogenation of the formed double bond.[69] It has to be noted that a proper design of the experimental setup and careful selection of the reaction parameters for consecutive reactions is required.[84]

Conclusion

The here presented techniques are powerful and mature tools to determine reaction rate constants and activation parameters

$\Delta G^{\ddagger}$, $\Delta H^{\ddagger}$ and $\Delta S^{\ddagger}$ for a broad range of reactions including the stereodynamics of molecules (e.g. rotation barriers of disubstituted BIPHEPs and small 1,2-dialkyldiaziridines) as well as first- and higher-order reactions. These techniques represent flexible yet highly efficient approaches to accommodate the needs of modern day synthesis development. Combining reaction, separation and analysis in a single setup offers not only a highly time- and labour-efficient approach but is also economically and environmentally friendly by saving supplies and solvents. The possibility of performing these studies in a high-throughput fashion only underlines the enormous potential for future applications.

Acknowledgement

Generous financial support by the European Research Council (ERC) for a Starting Grant (No. 258740, AMPCAT) is gratefully acknowledged.

Notes and references

[a] Organisch-Chemisches Institut, Ruprecht-Karls-Universität Heidelberg, Im Neuenheimer Feld 270, 69120 Heidelberg, Germany.
Fax: +49-6221-544904; E-Mail: trapp@oci.uni-heidelberg.de

1 J.-M. Lehn, *Angew. Chem.*, 2013, **125**, 2906-2921; *Angew. Chem. Int. Ed.*, 2013, **52**, 2836-2850.
2 T. D. Vu, A. Seidel-Morgenstern, S. Grüner and A. Kienle, *Industrial & Engineering Chemistry Research*, 2005, **44**, 9565-9574.
3 S. J. Haswell and P. Watts, *Green Chem.*, 2003, **5**, 240-249.
4 S. J. Haswell and V. Skelton, *Trends Anal. Chem.*, 2000, **19**, 389-395.
5 G. Jas and A. Kirschning, *Chem. Eur. J.*, 2003, **9**, 5708-5723.
6 P. Watts and S. J. Haswell, *Chem. Soc. Rev.*, 2005, **34**, 235.246.
7 F. E. Valera, M. Quaranta, A. Moran, J. Blacker, A. Armstrong, J. T. Cabral and D. G. Blackmond, *Angew. Chem.*, 2010, **122**, 2530-2537; *Angew. Chem. Int. Ed.*, 2010, **49**, 2478-2485.
8 C. Wiles and P. Watts, *Chem. Commun.*, 2011, **47**, 6512.
9 D. Webb and T. F. Jamison, *Chem. Sci.*, 2010, **1**, 675.
10 K. Jähnisch, V. Hessel, H. Löwe and M. Baerns, *Angew. Chem.*, 2004, **116**, 410-451; *Angew. Chem. Int. Ed.*, 2004, **43**, 406-446.
11 J. Wegner, S. Ceylan and A. Kirschning, *Chem. Commun.*, 2011, **47**, 4583.
12 O. Flögel, J. D. C. Codée, D. Seebach and P. H. Seeberger, *Angew. Chem.*, 2006, **118**, 7157-7160; *Angew. Chem. Int. Ed.*, 2006, **45**, 7000-7003.
13 N. Nikbin, M. Ladlow and S. V. Ley, *Org. Proc. Res. Dev.*, 2007, **11**, 458-562.
14 S. L. Bourne, P. Koos, M. O'Brien, B. Martin, B. Schenkel, I. R. Baxendale and S. V. Ley, *Synlett*, 2011, **18**, 2643-2647.
15 J. S. Moore and K. F. Jensen, *Angew. Chem. Int. Ed.*, 2014, **53**, 470.
16 J. Knight, *Nature*, 2002, **418**, 474-475.
17 D. Janasek, J. Franzke and A. Manz, *Nature*, 2006, **442**, 374-380.
18 S. J. Haswell, *Nature*, 2006, **441**, 705.
19 S. Fritzsche, S. Ohla, P. Glaser, D. S. Giera, M. Sickert, C. Schneider and D. Belder, *Angew. Chem.*, 2011, **123**, 9639-9642; *Angew. Chem. Int. Ed.*, 2011, **50**, 9467-9470.
20 D. Belder, *Anal. Bioanal. Chem.*, 2006, **385**, 416-418.
21 C. de Bellefon, N. Tanchoux, S. Caravieilhes, P. Grenouillet and V. Hessel, *Angew. Chem.*, 2000, **112**, 3584-3587; *Angew. Chem. Int. Ed.*, 2000, **39**, 3442-3445.
22 H. R. Sahoo, J. G. Kralj and K. F. Jensen, *Angew. Chem.*, 2007, **119**, 5806-5810; *Angew. Chem. Int. Ed.*, 2007, **46**, 5704-5708.
23 T. Noël, S. Kuhn, A. J. Musacchio, K. F. Jensen and S. L. Buchwald, *Angew. Chem.*, 2011, **123**, 6065-6068; *Angew. Chem. Int. Ed.*, 2011, **50**, 5943-5946.
24 J. Kobayashi, Y. Mori, K. Okamoto, R. Akiyama, M. Ueno, T. Kitamori and S. Kobayashi, *Science*, 2004, **304**, 1305-1308.
25 J.S. Rossier, N. Youhnovski, N. Lion, E. Damoc, S. Becker, F. Reymond, H.H. Girault and M. Przybylski, *Angew. Chem.*, 2003, **115**, 55-60; *Angew. Chem. Int. Ed.*, 2003, **42**, 53-58.
26 K. Grob, *Making and Manipulating Capillary Columns for Gas Chromatography*, Dr. Alfred Hüthig Verlag, Heidelberg, Basel, New York, 1986.
27 O. Trapp, G. Schoetz and V. Schurig, *Chirality*, 2001, **13**, 403-414.
28 C. Wolf, *Chem. Soc. Rev.*, 2005, **34**, 595-608.
29 I. D'Acquarica, F. Gasparrini, M. Pierini, C. Villani and G. Zappia, *J. Sep. Sci.*, 2006, **29**, 1508-1516.
30 C. Wolf, in *Dynamic Stereochemistry of Chiral Compounds - Principles and Applications*; RSC Publishing: Cambridge, 2008.
31 O. Trapp, *Electrophoresis* 2010, **31**, 789-813.
32 O. Trapp, *Chemistry Today*, 2008, **26**, 26-28.
33 G. Schoetz, O. Trapp and V. Schurig, *Enantiomer*, 2000, **5**, 391-396.
34 G. Schoetz, O. Trapp and V. Schurig, *Anal. Chem.*, 2000, **72**, 2758-2764.
35 G. Schoetz, O. Trapp and V. Schurig, *Electrophoresis* 2001, **22**, 3185-3190.
36 O. Trapp, G. Trapp and V. Schurig, *J. Biochem. Biophys. Methods*, 2002, **54**, 301-313.
37 O. Trapp, *Electrophoresis*, 2005, **26**, 487-493.
38 O. Trapp, *Electrophoresis*, 2006, **27**, 2999-3006.
39 N. A. Katsanos, R. Thede and F. Roubani-Kalantzopoulou, *J. Chromatogr. A*, 1998, **795**, 133-185.
40 K. Tamaru, *Nature*, 1959, **183**, 319-210.
41 D. W. Bassett and H. W. Habgood, *J. Phys. Chem.*, 1960, **64**, 769-773.
42 E. Gil-Av and Y. Herzberg-Minzly, *Proc. Chem. Soc.*, 1961, 316.
43 G. L. Pratt and S. H. Langer, *J. Phys. Chem.*, 1969, **73**, 2095-2097.
44 P. J. Marriott and Y.-H. Lai, *Inorg. Chem.*, 1986, **25**, 3680-3683.
45 J. M. Matsen, J. W. Harding and E. M. Magee, *J. Phys. Chem.*, 1965, **69**, 552-527.
46 P. J. Skrdla, *J. Chem. Kinet.*, 2004, **36**, 386-393.
47 L. C. Craig, *J. Biol. Chem.*, 1944, **155**, 519-534.
48 A. J. P. Martin and R. L. M. Synge, *Biochem. J.*, 1941, **35**, 1358-1368.
49 J. Kallen and E. Heilbronner, *Helv. Chim. Acta*, 1960, **43**, 489-500.
50 V. Schurig, W. Bürkle, A. Zlatkis and C.F. Poole, *Naturwissenschaften*, 1979, **66**, 423-424.
51 M. Jung and V. Schurig, *J. Am. Chem. Soc.*, 1992, **114**, 529-534.
52 W. Bürkle, H. Karfunkel and V. Schurig, *J. Chromatogr.*, 1984, **288**, 1-14.
53 O. Trapp and V. Schurig, *J. Am. Chem. Soc.*, 2000, **122**, 1424-1430.
54 O. Trapp and V. Schurig, *Comput. Chem*, 2001, **25**, 187-195.
55 O. Trapp, *Anal. Chem.*, 2006, **78**, 189-198.
56 O. Trapp, *Chirality*, 2006, **18**, 489-497.
57 F. Maier and O. Trapp, *Angew. Chem.*, 2012, **124**, 3039-3043; *Angew. Chem. Int. Ed.*, 2012, **51**, 2985-2988.
58 F. Maier and O. Trapp, *Chirality*, 2013, **25**, 126-132.
59 F. Maier and O. Trapp, *Angew. Chem.*, 2014, **126**, in press; *Angew. Chem. Int. Ed.*, 2014, **53**, in press.
60 M. Rieger and H. Westheimer, *J. Am. Chem. Soc.*, 1950, **72**, 19-28.
61 J. D. Dunitz, *Chem Biol*, 1995, **2**, 709-712.
62 O. Trapp, V. Schurig and R. G. Kostyanovsky, *Chem. Eur. J.*, 2004, **10**, 951-957.
63 R. G. Kostyanovsky, R. Murugan and M. Sutharchanadevi, in *Comprehensive Heterocyclic Chemistry II*, eds. A. R. Katritzky, C. W. Rees and E. F. V. Scriven, Pergamon, Oxford, 1996, pp. 347-364.
64 O. Trapp, *J. Chromatogr. A*, 2010, **1217**, 1010-1016.
65 M. Kamuf and O. Trapp, *Chirality*, 2011, **23**, 113-117.
66 M. Kamuf and O. Trapp, *Chirality*, 2013, **25**, 224-229.
67 D.G. Blackmond, *Angew. Chem.*, 2005, **117**, 4374-4393; *Angew. Chem. Int. Ed.*, 2005, **44**, 4302-4320.
68 O. Trapp, S. K. Weber, S. Bauch, T. Bäcker, W. Hofstadt and B. Spliethoff, *Chem. Eur. J.*, 2008, **14**, 4657-4666.
69 O. Trapp, S. K. Weber, S. Bauch and W. Hofstadt, *Angew. Chem.*, 2007, **119**, 7447-7451; *Angew. Chem. Int. Ed.*, 2007, **46**, 7307-7310.
70 M. R. an der Heiden, H. Plenio, S. Immel, E. Burello, G. Rothenberg and H. C. J. Hoefsloot, *Chem. Eur. J.*, 2008, **14**, 2857.
71 H. F. M. Boelens, D. Iron, J. A. Westerhuis and G. Rothenberg, *Chem. Eur. J.*, 2003, **9**, 3876.

72 S. Fuessl and O. Trapp, *Electrophoresis* 2012, **33**, 1060-1067.
73 J. Troendlin, J. Rehbein, M. Hiersemann and O. Trapp, *J. Am. Chem. Soc.*, 2011, **133**, 16444-16450.
74 V. Schurig, D. Schmalzing and M. Schleimer, *Angew. Chem.*, 1991, **103**, 994-996; *Angew. Chem. Int. Ed.*, 1991, **30**, 987-989.
75 H. Cousin, O. Trapp, V. Peulon-Agasse, X. Pannecoucke, L. Banspach, G. Trapp, Z. Jiang, J.C. Combret and V. Schurig, *Eur. J. Org. Chem.*, 2003, 3273-3287.
76 J. Gmeiner, M. Seibicke, C. Lang, U. Gärtner, O. Trapp, *Adv. Syn. Cat.* 2014, **356**, 2081-2087.
77 C. Lang, U. Gärtner, O. Trapp, *Chem. Commun.* 2011, **47**, 391-393.
78 S. C. Schürer, S. Gessler, N. Buschmann, S. Blechert, *Angew. Chem.* 2000, **112**, 4062-4065; *Angew. Chem. Int. Ed.* 2000, **39**, 3898-3901.
79 M. S. Sanford, J. A. Love, R. H. Grubbs, *J. Am. Chem. Soc.* 2001, **123**, 6543-6554.
80 S. Stockinger and O. Trapp, *Beilstein J. Org. Chem.*, 2013, **9**, 1837-1842.
81 S. Stockinger, O. Trapp, *Chirality* 2014, **26**, 243-248.
82 J. V. Seeley and S. K. Seeley, *Anal. Chem.*, 2013, **85**, 557-578.
83 S.-T. Chin, B. Maikhunthod and P. J. Marriott, *Anal. Chem.*, 2011, **83**, 6485-6492
84 D. Iron, H. F. M. Boelens, J. A. Westerhuis and G. Rothenberg, *Anal. Chem.*, 2003, **75**, 6701.

